arXiv:0801.2833v2 [nlin.CD] 5 May 2008

Dynamical tunneling in mushroom billiards

A. Bäcker, R. Ketzmerick, and S. Löck
Institut für Theoretische Physik, Technische Universität Dresden, D-01062 Dresden, Germany

M. Robnik and G. Vidmar
Center for Applied Mathematics and Theoretical Physics,
University of Maribor, SI-2000 Maribor, Slovenia

R. Höhmann, U. Kuhl, and H.-J. Stöckmann
Fachbereich Physik, Philipps-Universität Marburg, D-35032 Marburg, Germany

(Dated: May 5, 2008)

We study the fundamental question of dynamical tunneling in generic two-dimensional Hamiltonian systems by considering regular-to-chaotic tunneling rates. Experimentally, we use microwave spectra to investigate a mushroom billiard with adjustable foot height. Numerically, we obtain tunneling rates from high precision eigenvalues using the improved method of particular solutions. Analytically, a prediction is given by extending an approach using a fictitious integrable system to billiards. In contrast to previous approaches for billiards, we find agreement with experimental and numerical data without any free parameter.

PACS numbers: 05.45.Mt, 03.65.Sq, 03.65.Xp

Typical Hamiltonian systems have a mixed phase space in which regular and chaotic motion coexist. While classically these regions are separated, quantum mechanically they are coupled by tunneling. This process has been called “dynamical tunneling” [1] as it occurs across a dynamically generated barrier in phase space. Tunneling has been studied between symmetry related regular regions (chaos-assisted tunneling) [2, 3, 4, 5, 6, 7] and from a single regular region to the chaotic sea [8, 9, 10, 11, 12]. In contrast to the well understood 1D tunneling through a barrier, the quantitative prediction of dynamical tunneling is a major challenge. Results have been found for specific systems or system classes only, e.g. recently for 2D quantum maps with an approach using a fictitious integrable system [12]. However, a precise knowledge of tunneling rates is of great importance. Recent examples are spectral statistics in systems with a mixed phase space [13], eigenstates affected by flooding of regular islands [14], and emission properties of optical micro-cavities [15].

Billiards are an important class of Hamiltonian systems. Classically, a point particle moves along straight lines inside a domain with elastic reflections at its boundary. Quantum-mechanical approaches for dynamical tunneling rates have so far escaped a full quantitative prediction as they required fitting by a factor of 6 for the annular billiard [3] and by a factor of 100 (see below) for the mushroom billiard [16].

In this paper we present a combined experimental, theoretical, and numerical investigation of dynamical tunneling rates in mushroom billiards [17], which are of great current interest [13, 16, 18, 19, 20] due to their sharply divided phase space. Experiments are performed using a microwave cavity. Extending the approach using a fictitious integrable system [12] to billiards, we find quantitative agreement in the experimentally accessible regime, see Fig. 1, without a free parameter. In addition, numerical computations verify the predictions over 18 orders of magnitude with errors typically smaller than a factor of 2, see Fig. 4. The theoretical approach thus provides unprecedented agreement for tunneling rates in billiards.

We consider the desymmetrized mushroom billiard, i.e. the 2D autonomous system $H(\mathbf{p},\mathbf{q}) = \mathbf{p}^2/2M + V(\mathbf{q})$ shown in Fig. 2b, characterized by the radius of the quarter circle R, the foot width a and the foot height l. The potential is zero inside the domain Ω and infinite outside. Classically one has regular and chaotic dynamics as visualized by the phase-space portrait in Fig. 2d. Quantum mechanically the billiard is described by the time-independent Schrödinger equation $-\Delta\psi(\mathbf{q}) = E\psi(\mathbf{q})$ with Dirichlet boundary conditions at $\partial\Omega$, using the nat-

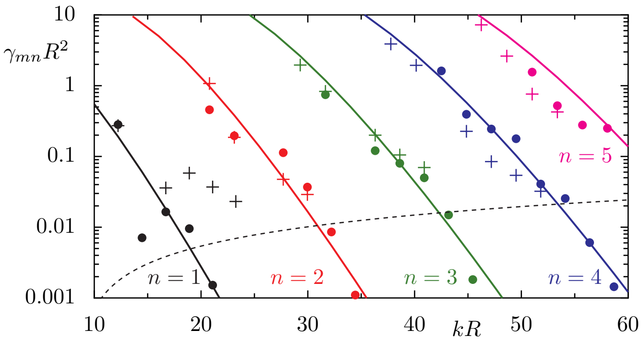

FIG. 1: (color online) Dynamical tunneling rates from the regular region to the chaotic sea for quantum numbers $n \leq 5$ vs kR for a mushroom billiard ($a/R = 10/19$): theoretical predictions (connected by solid lines) from Eq. (8), experimental results (crosses), and numerical data (dots). The dashed line denotes the lower limit of the experimental resolution.

ural units $2M = \hbar = 1$. The eigenstates can be classified as being either mainly regular or mainly chaotic, depending on the phase space region on which they concentrate.

The initial tunneling decay of a purely (unperturbed) regular state, is, according to Fermi's golden rule, described by a rate

$$\gamma = 2\pi \langle |v|^2 \rangle \rho_{\text{ch}}, \tag{1}$$

where $\langle |v|^2 \rangle$ is the averaged squared matrix element between this regular state and the chaotic states of similar energy. According to Weyl's formula the density of chaotic states is $\rho_{\text{ch}} \approx A_{\text{ch}}/4\pi$, where $A_{\text{ch}} = la + [R^2 \arcsin(a/R) + a\sqrt{R^2 - a^2}]/2$ is the area of the billiard times the fraction of the chaotic phase-space volume.

Under variation of the foot height l (and for not too large ρ_{ch} [14]) avoided crossings of this regular state with different chaotic states are observable. The splittings $\Delta E = 2|v|$ determine individual matrix elements for different billiards with varying ρ_{ch}. We therefore extend the average in Eq. (1) also over ρ_{ch} relying on the assumption that the regular-to-chaotic tunneling rate γ is a local property of the hat region, where the regular phase-space component resides, and thus does not depend on the foot height. This leads to

$$\gamma = \langle |\Delta E|^2 A_{\text{ch}}/8 \rangle, \tag{2}$$

where A_{ch} in the experiment varies from 0.5 to 1.2 when increasing l from 0 to 25.7 cm.

Fig. 2a shows the mushroom billiard used in the microwave experiment. Spectra have been taken as a function of the foot height l of the mushroom in the frequency regime 3.0 to 13.5 GHz, corresponding to values of kR between 11.9 and 53.8. Fig. 3 shows part of the obtained spectra in a small kR window. As the energy of the regular states of the quarter circle do not depend on the foot height, they appear as straight horizontal lines, whereas the chaotic states are shifted to lower energies with increasing foot height l, reflecting the increasing density ρ_{ch} of chaotic states.

For each of the regular states, see Eq. (4), with radial quantum numbers n between 1 and 5, and azimuthal quantum numbers m even between 8 and 32 all accessible splittings at avoided crossing Δk have been determined by means of a hyperbola fit (Fig. 3). From this we get the energy splittings $\Delta E = 2k\Delta k$ of the corresponding quantum system and by averaging over all avoided crossings, Eq. (2), deduce the tunneling rates γ_{mn} from regular states (m, n) to the chaotic sea. Apart from the results for $n = 1$ they are in very good agreement with the theoretical prediction, Eq. (8), derived below.

The experimental resolution of avoided crossings is limited by the line widths of the resonances caused by wall absorption and antenna coupling. In the studied frequency regime the line widths were about $\Delta\nu_w = 0.01$ GHz, corresponding to a $\Delta k_w R \approx 0.004$. From the hyperbola fit of the avoided crossings all splittings ΔkR larger than $0.1\Delta k_w R$ could still be resolved, corresponding to tunneling rates γ between 0.001 and 0.024, see Fig. 1 (dashed line). Another complication is caused by the antenna giving rise to an additional splitting [13], which is proportional to the product of the involved wave functions $|\psi(\mathbf{q}_a)|$ at the antenna position $\mathbf{q}_a$. For the rightmost three data points for $n = 1$, see Fig. 1, $|\psi_{\text{reg}}^{m1}(\mathbf{q}_a)|$ is particularly large, which is probably the explanation for the deviations between experiment and theory observed in these cases.

Now we derive a formula for tunneling rates in billiards. This faces a general problem: The matrix element v, appearing in Eq. (1), cannot be calculated from the nominally regular and chaotic eigenstates of H, as they have small, but still too large, admixtures of the other type of states. Instead, we determine v by introducing a fictitious regular billiard system H_{reg} with purely regular eigenstates, extending an approach for 1D quantum maps [12]. H_{reg} has to be chosen such that its classical dynamics resembles the classical motion corresponding to H within the regular region as closely as possible. The eigenstates ψ_{reg} of H_{reg} are localized in the regular region and continue to decay into the chaotic sea. With states ψ_{ch} living in the chaotic region of phase space, we use in analogy to Ref. [12] for the coupling matrix element

$$v = \int_\Omega \psi_{\text{ch}}^*(x, y)(H - H_{\text{reg}})\psi_{\text{reg}}(x, y)\, \mathrm{d}x\, \mathrm{d}y. \tag{3}$$

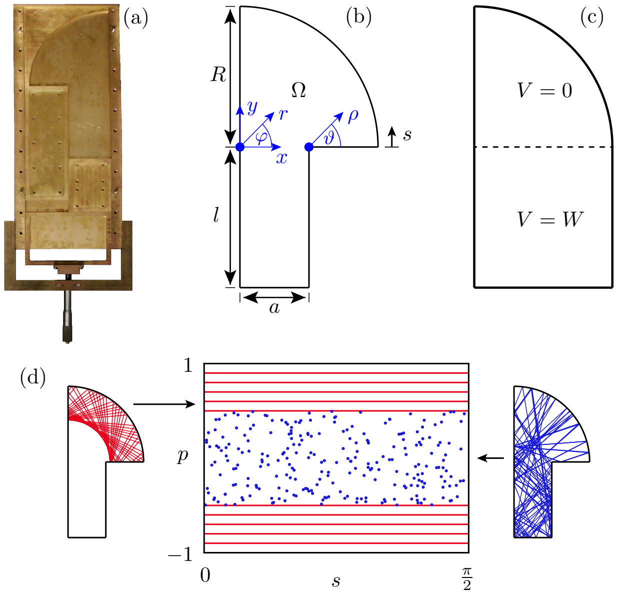

FIG. 2: (a) Experimental desymmetrized mushroom billiard with radius $R = 19$ cm, foot width $a = 10$ cm and foot height $l = 0 \dots 25.7$ cm. The antenna is located 4 cm below the top and has a distance of 0.75 cm from the vertical wall. (b) Schematic picture showing the coordinate systems used in the theoretical derivation. (c) Auxiliary billiard H_{reg}^W. (d) Phase-space portrait at the quarter circle boundary (relative tangential momentum p vs arclength s) showing regular and chaotic regions with illustrations of trajectories.

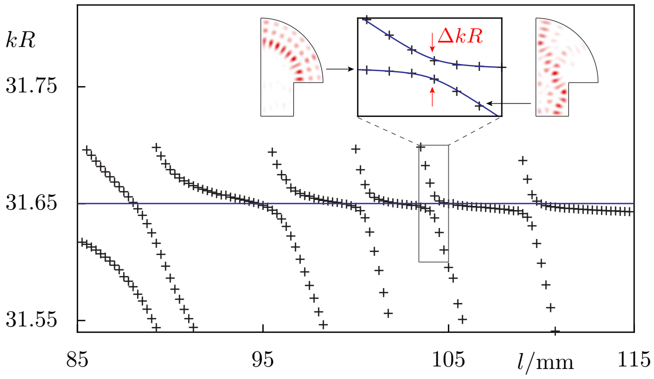

FIG. 3: (color online) Part of the evaluated experimental resonance spectra of the mushroom microwave billiard vs foot height l. The horizontal line corresponds to the eigenfrequency of $\psi_{\mathrm{reg}}^{18,3}$, the crosses mark the extracted resonances. The inset shows a magnification of one avoided crossing, including a hyperbola fit (solid line), and the numerically obtained regular and chaotic states involved in the crossing.

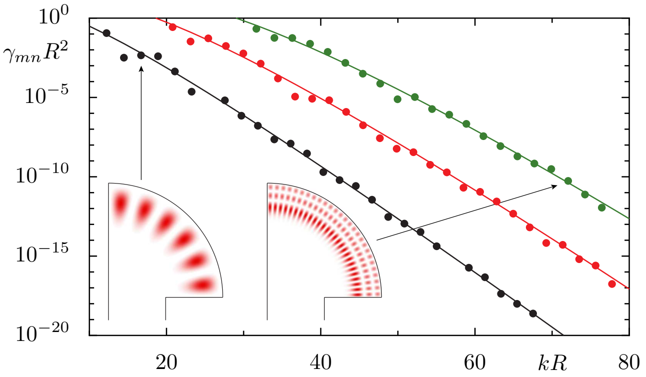

FIG. 4: (color online) Tunneling rates from regular states with quantum numbers $n = 1$, 2, and 3 vs kR for $a/R = 0.5$ comparing prediction Eq. (8) (connected by solid lines) and numerical data (dots). The insets show the regular eigenfunctions $\psi_{\mathrm{reg}}^{12,1}(x,y)$ and $\psi_{\mathrm{reg}}^{54,3}(x,y)$.

Eqs. (1) and (3) define our approach for determining dynamical tunneling rates in billiards. Note, that it requires the determination of reasonably good H_{reg} and ψ_{reg}, which for a general billiard is a difficult task.

We will now apply this approach to the desymmetrized mushroom billiard, see Fig. 2b. We set $R = 1$ in the following analysis. A natural choice for the regular system H_{reg} is the quarter-circle billiard with its eigenstates

$$\psi_{\mathrm{reg}}^{mn}(r,\varphi) = N_{mn} J_m\left(j_{mn} r\right) \sin(m\varphi), \tag{4}$$

in polar coordinates (r,φ). They are characterized by the radial ($n = 1, 2, \dots$) and the azimuthal ($m = 2, 4, \dots$) quantum numbers. Here J_m denotes the mth Bessel function, j_{mn} the nth root of J_m, $N_{mn} = \sqrt{8/\pi}/J_{m-1}(j_{mn})$ the normalization, and $E_{mn} = j_{mn}^2$ is the eigenenergy.

Evaluating Eq. (3) leads for $y \leq 0$ to the undefined product of $H - H_{\mathrm{reg}} = -\infty$ and $\psi_{\mathrm{reg}}^{mn} = 0$. We therefore introduce the auxiliary billiard H_{reg}^{W}, see Fig. 2c, with a large but finite potential $V(x, y \leq 0) = W \gg E$. We evaluate Eq. (3) in the limit $W \to \infty$, where H_{reg}^{W} approaches H_{reg}, leading to

$$\begin{aligned} v &= \lim_{W\to\infty} \int_0^a \mathrm{d}x \int_{-l}^0 \mathrm{d}y\, \psi_{\mathrm{ch}}(x,y)(-W)\psi_{\mathrm{reg},W}^{mn}(x,y) \\ &= -\int_0^a \mathrm{d}x\, \psi_{\mathrm{ch}}(x,y=0)\, \partial_y \psi_{\mathrm{reg}}^{mn}(x,y=0), \end{aligned} \tag{5}$$

where we performed the y-integration on $\psi_{\mathrm{reg},W}^{mn}(x,y) = \psi_{\mathrm{reg},W}^{mn}(x,y=0)\exp(\sqrt{W - E_{mn}}y)$, following from the Schrödinger equation for $y < 0$ and the continuity at $y = 0$. Furthermore we used $\partial_y \psi_{\mathrm{reg},W}^{mn}(x,y=0) = \sqrt{W - E_{mn}}\psi_{\mathrm{reg},W}^{mn}(x,y=0)$, following from the continuity of the derivative at $y = 0$, and we replaced $\lim_{W\to\infty}\sqrt{W}\exp(\sqrt{W - E_{mn}}y)$ by a Dirac delta function. Below we use $\partial_y \psi_{\mathrm{reg}}^{mn}(x,0) = m N_{mn} J_m(j_{mn}x)/x$.

For the chaotic states $\psi_{\mathrm{ch}}(x,y)$ we employ a random wave description [21], which has recently been extended to systems with a mixed phase space [22]. While this describes the behavior inside the billiard accurately, it would not include the effect of the boundary, e.g. near the corner, where the main contribution of the integral in Eq. (5) arises. We extend a boundary-adapted random wave model [23] to the case of a corner with angle $3\pi/2$ using basis states with Dirichlet boundary conditions [24],

$$\psi_{\mathrm{ch}}(\rho,\vartheta) \approx \sqrt{\frac{8}{3A_{\mathrm{ch}}}} \sum_{s=1}^{\infty} c_s J_{\frac{2s}{3}}\left(\sqrt{E}\rho\right) \sin\left(\frac{2s}{3}\vartheta\right), \tag{6}$$

where the polar coordinates (ρ,ϑ) at the corner are related to (x,y) by $x = a + \rho\cos(\vartheta)$ and $y = \rho\sin(\vartheta)$ (see Fig. 2b). The coefficients c_s of this ensemble are independent Gaussian random variables with $\langle c_s\rangle = 0$ and $\langle c_s c_t\rangle = \delta_{s,t}$. The normalization is chosen such that $\langle|\psi_{\mathrm{ch}}(\rho,\vartheta)|^2\rangle = 1/A_{\mathrm{ch}}$ holds far away from the corner. Note, that (i) we do not require these chaotic states to decay into the regular island, as Eq. (5) is an integral along a line of the billiard where the phase space is fully chaotic, and that (ii) near the boundary, but away from the corner, one recovers the behavior $1 - J_0(2k|x|)$ [23, 25]. Inserting Eq. (6) for $\vartheta = \pi$ into Eq. (5) one can determine the averaged squared matrix element, $\langle|v|^2\rangle$, and with Eq. (1) one gets

$$\gamma_{mn} = m^2 N_{mn}^2 {\sum_{s=1}^{\infty}}' \left[\int_0^a \frac{\mathrm{d}x}{x} J_m(j_{mn}x) J_{\frac{2s}{3}}(j_{mn}[a\text{-}x])\right]^2, \tag{7}$$

where the sum over s excludes all multiples of 3, which is indicated by the prime. The remaining integral can be solved analytically, leading to

$$\gamma_{mn} = \frac{8}{\pi} \sum_{s=1}^{\infty}{}' \frac{J_{m+\frac{2s}{3}}(j_{mn}a)^2}{J_{m-1}(j_{mn})^2} \tag{8}$$

for the tunneling rates from any regular state ψ_{reg}^{mn} in the mushroom billiard. The sum has its dominant contribution for $s = 1$ and using $s \leq 2$ is sufficiently accurate.

It is worth to remark that a very plausible estimate of the tunneling rate is given by the averaged square of the regular wave function on a circle with radius a, i.e. the boundary to the fully chaotic phase space, yielding $\gamma_{mn}^0 = N_{mn}^2 J_m(j_{mn}a)^2/2$. Surprisingly, it is just about a factor of 2 larger for the parameters we studied. In Ref. [16] a related quantity is proposed, given by the integral of the squared regular wave function over the quarter circle with radius a. This quantity, however, is too small by a factor of order 100 for the parameters under consideration.

The eigenvalues and eigenfunctions of the mushroom billiard are determined by numerically solving the Schrödinger equation. Because of its superior computational efficiency we have chosen to use the improved method of particular solutions [16, 26] allowing a determination of the energies E with a relative error $\approx 10^{-14}$. Analyzing avoided crossings of a given regular state with typically 30 chaotic states we deduce from Eq. (2) the tunneling rate. Note, that some pairs of regular states are very close in energy, e.g. $E_{20,1} - E_{16,2} \approx 10^{-4}$, such that their avoided crossings with a chaotic state overlap, making a numerical determination of the smaller tunneling rate unfeasible within the presented approach. Fig. 4 shows the tunneling rates γ_{mn} for fixed radial quantum number $n = 1, 2, 3$ and increasing azimuthal quantum number m, comparing the theoretical prediction, Eq. (8), with numerical results. We find excellent agreement for tunneling rates γ_{mn} over 18 orders of magnitude.

In the experiment the unavoidable coupling to the environment dominates for small tunneling rates, but Fig. 1 shows, that in the microwave experiment the coupling by the antenna is negligible over three orders of magnitude. This is a promising aspect for future experimental studies of more complex systems, in particular when numerical and theoretical results are not available.

In summary, we have presented an experimental, numerical, and theoretical investigation of tunneling rates in the mushroom billiard. We find agreement without any free parameter, which is unprecedented for billiards. This success of the approach using a fictitious integrable system gives confidence that in the future it can be applied to generic billiards, where the determination of a suitable H_{reg} is more challenging.

We thank the DFG for support within the Forschergruppe 760 “Scattering Systems with Complex Dynamics”, the cooperation program between the Universities of Marburg and Maribor, the Ministry of Higher Education, Science and Technology of the Republic of Slovenia, and R. K. thanks the Kavli Institute for Theoretical Physics at UCSB (NSF Grant No. PHY05-51164).

---

[1] M. J. Davis and E. J. Heller, J. Chem. Phys. **75**, 246 (1981).
[2] O. Bohigas, S. Tomsovic, and D. Ullmo, Phys. Rep. **223**, 43 (1993).
[3] E. Doron and S. D. Frischat, Phys. Rev. Lett. **75**, 3661 (1995); S. D. Frischat and E. Doron, Phys. Rev. E **57**, 1421 (1998).
[4] C. Dembowski et al., Phys. Rev. Lett. **84**, 867 (2000).
[5] D. A. Steck, W. H. Oskay, and M. G. Raizen, Science **293**, 274 (2001).
[6] W. K. Hensinger et al., Nature **412**, 52 (2001).
[7] O. Brodier, P. Schlagheck, and D. Ullmo, Phys. Rev. Lett. **87**, 064101 (2001); Ann. Phys. **300**, 88 (2002); C. Eltschka and P. Schlagheck, Phys. Rev. Lett. **94**, 014101 (2005).
[8] J. D. Hanson, E. Ott, and T. M. Antonsen, Phys. Rev. A **29**, 819 (1984).
[9] A. Shudo and K. S. Ikeda, Phys. Rev. Lett. **74**, 682 (1995)
[10] M. Sheinman, S. Fishman, I. Guarneri, and L. Rebuzzini, Phys. Rev. A **73**, 052110 (2006).
[11] J. Feist, A. Bäcker, R. Ketzmerick, S. Rotter, B. Huckestein, and J. Burgdörfer, Phys. Rev. Lett. **97**, 116804 (2006).
[12] A. Bäcker, R. Ketzmerick, S. Löck, and L. Schilling, Phys. Rev. Lett. **100**, 104101 (2008).
[13] G. Vidmar, H.-J. Stöckmann, M. Robnik, U. Kuhl, R. Höhmann, and S. Grossmann, J. Phys. A **40**, 13883 (2007).
[14] A. Bäcker, R. Ketzmerick, and A. G. Monastra, Phys. Rev. Lett. **94**, 054102 (2005); Phys. Rev. E **75**, 066204 (2007).
[15] J. Wiersig and M. Hentschel, Phys. Rev. Lett. **100**, 033901 (2008).
[16] A. H. Barnett and T. Betcke, Chaos **17**, 043125 (2007).
[17] L. A. Bunimovich, Chaos **11**, 802 (2001).
[18] E. G. Altmann, A. E. Motter, and H. Kantz, Chaos **15**, 033105 (2005).
[19] H. Tanaka and A. Shudo, Phys. Rev. E **74**, 036211 (2006).
[20] B. Dietz, T. Friedrich, M. Miski-Oglu, A. Richter, and F. Schäfer, Phys. Rev. E **75**, 035203(R) (2007).
[21] M. V. Berry, J. Phys. A **10**, 2083 (1977).
[22] A. Bäcker and R. Schubert, J. Phys. A **35**, 527 (2002).
[23] M. V. Berry, J. Phys. A **35**, 3025 (2002).
[24] R. S. Lehman, J. Math. Mech. **8**, 727 (1959).
[25] A. Bäcker, R. Schubert, and P. Stifter, Phys. Rev. E **57**, 5425 (1998).
[26] T. Betcke and L. N. Trefethen, SIAM Review **47**, 469 (2005).